

Non-zero macroscopic magnetization in half-metallic antiferromagnets at finite temperatures

Ersoy Şaşıoğlu*

*Institut für Festkörperforschung, Forschungszentrum Jülich, D-52425 Jülich, Germany
and Department of Physics, Fatih University, Büyükçekmece, TR-34500, İstanbul, Turkey*

(Dated: February 4, 2022)

Combining density functional theory calculations with many-body Green function technique, we reveal that the macroscopic magnetization in half-metallic antiferromagnets does not vanish at finite temperature as for the $T = 0$ limit. This anomalous behavior stems from the inequivalent magnetic sublattices which lead to different intra-sublattice exchange interactions. As a consequence, the spin fluctuations suppress the magnetic order of the sublattices in a different way leading to a ferrimagnetic state at finite temperatures. Computational results are presented for the half-metallic antiferromagnetic CrMnZ ($Z = \text{P, As, Sb}$) semi-Heusler compounds.

PACS numbers: 75.50.Cc, 75.30.Et, 71.15.Mb, 75.60.-d

Half-metallic antiferromagnets (HM-AFMs) are considered to be the most promising class of materials for spintronics applications.^{1,2} A HM-AFM material is not antiferromagnetic in the usual sense of the term; it is a special case of a ferrimagnet with compensated sublattice magnetization. The existence of the gap in one of the spin channels (either up or down) leads to the complete cancellation of the magnetic moments at zero temperature with a 100% spin polarization of the charge carriers at the Fermi level. In conventional AFMs the macroscopic spin polarization is zero due to the spin rotational symmetry with the exception of the compounds with broken inversion symmetry like $\alpha\text{-Fe}_2\text{O}_3$ in which spin-orbit gives rise to weak ferromagnetism ($0.002 \mu_B$) due to the canting of the magnetic moments.^{3,4} The HM-AFM materials provide several advantages in device applications with respect to the half-metallic ferromagnets (HM-FMs). For example, they would be perfectly stable spin-polarized electrodes in a junction device. These materials do not give rise to stray fields, and thus no magnetic domain walls are formed. Besides applications in spintronics, HM-AFMs provide a possibility of "single spin superconductivity" due to the spin triplet ($S = 1$) pairing in metallic channel.⁵

The possible existence of HM-AFM was pointed out by van Leuken and de Groot in 1995.⁶ Based on first-principles calculations authors proposed CrMnSb and $\text{V}_7\text{MnFe}_8\text{Sb}_7\text{In}$ as candidates for HM-AFMs. Later, Pickett suggested that also the cubic double perovskites La_2VCuO_6 , La_2MnVO_6 , and $\text{La}_2\text{MnCoO}_6$ are HM-AFMs.⁷ Since then substantial effort has been devoted to find materials with HM antiferromagnetic characteristics. Predicted promising systems include double perovskites^{8,9}, thiospinels¹⁰, tetrahedrally coordinated transition-metal-based chalcopyrites¹¹, full-Heusler alloys^{12,13} and monolayer superlattices.¹⁴ Not only ordered but also several disordered systems have been shown to be HM-AFMs.^{15,16,17,18,19,20} In spite of substantial theoretical efforts for designing materials with HM-AFM characteristics and the study of their ground state electronic and magnetic properties, only

few works exist addressing the exchange interactions and magnetic phase transition temperatures in these systems.^{19,20}

In this Communication we investigate the temperature dependence of the magnetization in HM-AFMs employing the many-body Green function technique²¹ within Tyablikov decoupling scheme.²² For computational purposes we consider CrMnZ ($Z = \text{P, As, Sb}$) semi-Heusler compounds which are the simplest systems among the predicted HM-AFMs with two magnetic atoms per unit cell and which are compatible with the existing semiconductors technology. However, present findings are valid for more complicated systems like double perovskites^{8,9} or diluted antiferromagnetic semiconductors.^{19,20} We show that the macroscopic magnetization in these materials does not vanish at finite temperature in contrast to the zero temperature limit and conventional AFMs. This peculiar behavior originates from the inequivalent magnetic sublattices in HM-AFMs which lead to different intra-sublattice exchange interactions and, as a consequence, spin fluctuations suppress the magnetic order of the sublattices in a different way. Thus, at finite temperature sublattice magnetizations do not compensate each other and all three compounds show ferrimagnetic behavior which seems to be contradictory to our knowledge on finite temperature properties of the magnetic materials. However, this seemingly counterintuitive results can be explained by an analysis of the electronic structure and exchange interactions in these systems.

Ground state calculations are carried out using the augmented spherical wave method within the generalized gradient approximation to the exchange correlation potential. Details of the computational scheme can be found in Ref. 23. To provide the basis for further considerations we start with a brief discussion of the electronic structure of the CrMnZ compounds. Like several Heusler alloys these systems have theoretical equilibrium lattice constants (see Table I) close to the ones of the zincblende semiconductors (GaP, GaAs). Thus, calculational results will be presented for the latter case since these semiconductors might be considered as possible substrates

TABLE I: Lattice parameters and spin magnetic moments (in μ_B) for CrMnZ (Z = P, As, Sb). The calculated equilibrium lattice constants are 5.44 Å, 5.71 Å and 6.08 Å for Z = P, As and Sb, respectively, close to the experimental lattice parameters of GaP, GaAs and InP.

Compound	a(Å)	m _{Cr}	m _{Mn}	m _Z	m _{Cell}
CrMnP	5.45 _[GaP]	1.80	-1.83	0.03	0.00
CrMnAs	5.65 _[GaAs]	2.52	-2.54	0.02	0.00
CrMnSb	5.87 _[InP]	2.74	-2.76	0.02	0.00

to grow these materials.²⁴ All compounds under study have 18 valance electrons per unit cell and calculations show that the total spin moments given in Table I are exactly zero in agreement with the Slater-Pauling behavior for ideal half-metals.²⁵ Simultaneously, the spin magnetic moments of Cr and Mn atoms are antiparallel and these compounds are ferrimagnets with compensated sublattice magnetizations. The origin of the HM gap in Heusler alloys has been well understood and the reader is referred to Ref. 25 since the same discussion is valid for the present systems.

To study interatomic exchange interactions we map the complex itinerant electron problem onto a classical Heisenberg Hamiltonian $H = -\sum_{\mu,\nu} \sum_{\mathbf{R},\mathbf{R}'} J_{\mathbf{R}\mathbf{R}'}^{\mu\nu} s_{\mathbf{R}}^{\mu} s_{\mathbf{R}'}^{\nu}$ where $\mu\mathbf{R} \neq \nu\mathbf{R}'$ and the indices μ and ν represent different sublattices. \mathbf{R} and \mathbf{R}' are the lattice vectors specifying the atoms within the sublattices, and $s_{\mathbf{R}}^{\mu}$ is the unit vector pointing in the direction of the magnetic moment at site (μ, \mathbf{R}) . Heisenberg exchange parameters $J_{\mathbf{R}\mathbf{R}'}^{\mu\nu}$ are calculated employing the frozen-magnon technique as described in Ref. 23. Extensive investigations on the multi-sublattice Heusler alloys have shown that there are several exchange interactions which coexist and which are mixed together.^{23,26,27,31} To simplify the discussion let us write the total magnetic exchange field acting on the sublattice μ as $J_{\text{total}}^{\mu} \sim J_{\text{direct}}^{(\mu\nu)} + J_{\text{indirect}}^{(\mu\nu)} + J_{\text{indirect}}^{(\mu\mu)}$ where the first two terms represent the direct and indirect exchange coupling between different sublattices. The former (direct coupling) provides the leading contribution to the total exchange coupling and determines the character of the magnetic state while the latter contributes little and is not so important. On the other hand, the last term, i.e., the intra-sublattice coupling is of particular importance because it is responsible for the appearance of a net macroscopic magnetization at finite temperature in HM-AFMs. It should be noted here that in reality the situation is not so simple, the exchange field acting on the sublattices should be determined from the solution of a matrix equation.

Let us start with the discussion of the last term. Because of the large distance between Cr-Cr (Mn-Mn) atoms this coupling is indirect mediated by the conduction electrons. In Fig. 1 we present the calculated Cr-Cr and Mn-Mn Heisenberg exchange parameters as a function of the distance. As seen, due to inequivalent

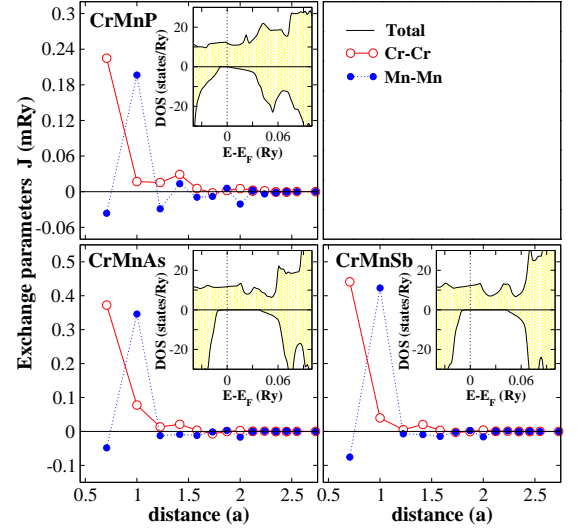


FIG. 1: (Color online) Intra-sublattice Cr-Cr and Mn-Mn exchange interactions in CrMnZ (Z = P, As, Sb) as a function of distance. In the insets we show spin-resolved total density of states around Fermi level.

magnetic sublattices the pattern of Cr-Cr and Mn-Mn exchange parameters show very different behavior. Although the former has ferromagnetic character, the latter shows oscillatory behavior so that the ferromagnetic and antiferromagnetic contributions partly compensate each other giving rise to a small contribution into the total exchange field acting on the Mn sublattice. In Table II we present the intra-sublattice ($J_0^{\mu} = \sum_{\mathbf{R} \neq 0} J_{0\mathbf{R}}^{\mu\mu}$) as well as the inter-sublattice ($J_0^{\mu\nu} = \sum_{\mathbf{R}} J_{0\mathbf{R}}^{\mu\nu}$) on-site exchange coupling parameters. The on-site Cr-Cr and Mn-Mn exchange couplings are rather different and this difference will be reflected as a net macroscopic magnetization at finite temperatures (see Fig. 2). It is worth to note that in conventional AFMs this coupling is the same for both sublattices. The increase of the strength of the exchange interactions and correspondingly of the critical temperatures in the P-As-Sb sequence can be explained by the increase of the magnetic moments (see Table I). Moreover, due to the presence of the HM gap the exchange interactions quickly decay.^{26,27}

In contrast to the intra-sublattice exchange interactions, the inter-sublattice (Cr-Mn) ones behave very differently. Due to the smaller Cr-Mn distance a very strong antiferromagnetic nearest-neighbor direct interaction takes place between these atoms which is about one order of magnitude larger than the nearest-neighbor Cr-Cr coupling and is responsible for the formation of the ferrimagnetic state. The interactions between further nearest neighbors are very small. The on-site Cr-Mn exchange couplings presented in Table II are about 4 and 20 times larger than the Cr-Cr and Mn-Mn ones, respectively. Note that the ferromagnetic intra-sublattice exchange interactions further stabilize the ferrimagnetic order. The antiferromagnetic coupling of the Cr and Mn atoms can be qualitatively explained on

TABLE II: On-site exchange parameters (in mRy) and estimated critical temperatures (in K) within RPA for quantum ($T_C^{[Q]}$) and classical ($T_C^{[C]}$) spins for CrMnZ (Z = P, As, Sb).

Compound	$J_0^{[Cr-Cr]}$	$J_0^{[Mn-Mn]}$	$J_0^{[Cr-Mn]}$	$T_C^{[Q]} (K)$	$T_C^{[C]} (K)$
CrMnP	3.80	0.03	-12.99	2530	1264
CrMnAs	5.55	0.84	-19.50	2610	1566
CrMnSb	5.96	1.06	-20.16	2986	1792

the basis of the following facts: First, half-filled shells tend to yield a strong trend towards antiferromagnetism and second, exchange coupling in 3d transition metals obeys the semi-phenomenological Bethe-Slater-Néel curve which predicts antiferromagnetism in the case of small interatomic distances.²⁸ Indeed, the Cr-Mn distance ($d_{[Cr-Mn]} = 2.36 - 2.54 \text{ \AA}$) in the present systems is comparable with the Cr-Cr distance ($d_{[Cr-Cr]} = 2.52 \text{ \AA}$) in the antiferromagnetic bcc Cr and both magnetic atoms possess half-filled 3d shells, thus, antiferromagnetic Cr-Mn coupling is expected.

With calculated exchange parameters in hand, now we can study temperature dependence of the magnetization employing the methods of statistical mechanics to the Heisenberg Hamiltonian. We use the many-body Green function technique²¹ within Tyablikov decoupling scheme²² [also known as the random-phase approximation (RPA)] as described in Ref. 31. Note that RPA takes into account only transverse spin fluctuations and the spin-flip Stoner excitations (longitudinal spin fluctuations) are neglected. However, available experimental data on Heusler alloys have shown that these latter excitations are well separated in energy from the former one (spin waves) due to large exchange splitting Δ ($\Delta \sim 2 - 3 \text{ eV}$).²⁹ In addition to this the presence of HM gap prevents spin-flip transitions. Thus, Stoner excitations do not play an important role in thermodynamics of the present systems and the RPA method is well grounded. We consider both classical-spin and quantum-spin cases. In the classical-spin calculations the obtained values of the magnetic moments (see Table I) are used while for the quantum mechanical case we assign integer values to the atomic moments: $2\mu_B$ ($S = 1$) (for Cr and Mn) in CrMnP and $3\mu_B$ ($S = 3/2$) in CrMnAs and CrMnSb. In quantum-spin case the thermal average of the sublattice magnetization is given by the Callen's expression³⁰

$$\langle \hat{s}_\mu^z \rangle = \frac{(S_\mu - \Phi_\mu)(1 + \Phi_\mu)^{2S_\mu+1} + (S_\mu + 1 + \Phi_\mu)\Phi_\mu^{2S_\mu+1}}{(1 + \Phi_\mu)^{2S_\mu+1} - (\Phi_\mu)^{2S_\mu+1}}$$

where Φ_μ is an auxiliary function. As the Φ_μ depends on the $\langle \hat{s}_\mu^z \rangle$ as well as $\langle \hat{s}_\nu^z \rangle$ to be determined, the above equation forms a self-consistency problem to be solved by iteration. Note that for classical spins the Callen's expression is reduced to the Langevin function.³¹ In Fig. 2 we present the calculated temperature dependence of the sublattice and total magnetization for CrMnZ (Z = P,

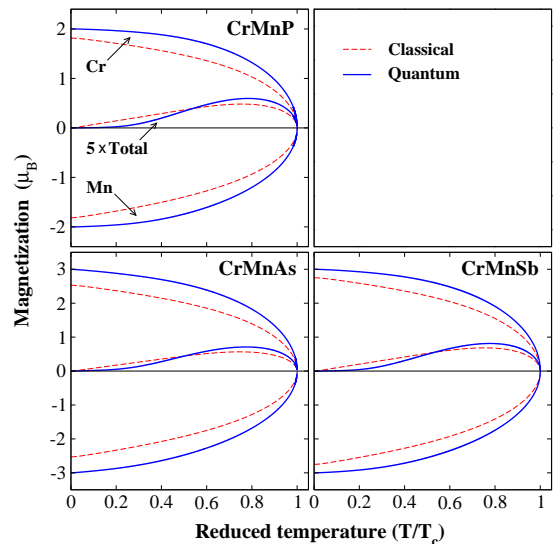


FIG. 2: (Color online) The calculated temperature dependence of the sublattice and total magnetization for CrMnZ (Z = P, As, Sb). The calculations are performed for both classical and quantum Hamiltonians. The temperature is given in reduced form and the total magnetization is scaled up by a factor of 5.

As, Sb). The temperature is given in reduced form and the total magnetization is scaled up by a factor of 5. As seen, the spin fluctuations suppress the magnetic order of the sublattices differently, i.e., the magnetization of the Mn sublattice decreases faster than the Cr one and as a result the total magnetization does not vanish at finite temperature in contrast to the $T = 0$ limit. This behavior can be traced back to the different exchange fields acting on the sublattices (see Table II). The total magnetization shows non-monotonous behavior i.e., first, it increases with increasing temperature up to $0.8 T_C$ and then decreases much faster and finally becomes zero at the critical point. For quantum mechanical case the calculated total magnetic moment around $0.8 T_C$ is $0.1 - 0.16\mu_B$ ($0.006 - 0.01\mu_B$ around room temperature) which is about two orders of magnitude larger than the spin-orbit coupling induced weak magnetic moment ($0.002 \mu_B$) in $\alpha\text{-Fe}_2\text{O}_3$.³ We should also note that in these systems not only the ideal case of zero macroscopic magnetization but also half-metallicity is limited to the $T = 0$.^{2,32,33}

The nature of the spin (quantum or classical) plays an important role in the temperature behavior of the magnetization curves. In the quantum case, the magnetization drops slower than the classical case and thus, the calculated T_C values are larger by a factor of $(S + 1)/S$ entering the RPA expression (see Ref. 31). Note that this factor becomes unity for classical spins ($(S + 1)/S \rightarrow 1$ for $S \rightarrow \infty$). Another important point which is outside the scope of the present work is that in both treatments we use the exchange parameters estimated within the picture of classical atomic moments. However, it is possible that the values of the exchange parameters must

be modified for the use in the quantum-mechanical calculations. In general, the classical calculation provides reasonable values of the critical temperature compared with experiment while the quantum mechanical treatment gives better form of the temperature dependence of the magnetization.³¹ The calculated critical temperatures within RPA are presented in Table II. We notice that the predicted T_C values of the CrMnAs and CrMnSb are even higher than the fcc Co which possesses the highest critical temperature (1400 K) among all known magnetic materials. This is not surprising, because available experimental and theoretical data have shown that the critical temperatures of HM ferromagnets (or ferrimagnets) scales linearly with the average value of the magnetic moment per atom in the unit cell.³⁴ In this respect Co_2FeSi possesses the largest average magnetic moment per atom of $1.5\mu_B$ with an experimental T_C of 1100 K. However, in CrMnAs (CrMnSb) the average value of the absolute magnetic moment per atom is $1.68\mu_B$ ($1.83\mu_B$) which is larger than the corresponding value in Co_2FeSi , and thus such high critical temperatures are expected. Finally we should note that so far discussion is based on the assumption that CrMnZ compounds possess C1_b -type ordered crystal structure and the effect of disorder is completely ignored. However, in reality disorder exist in various forms like defects, anti-sites or atomic

swaps which reduce not only the spin polarization at the Fermi level but also the magnetic phase transition temperature.³⁵ For example migration of the Cr atoms to the vacant sublattice is expected to reduce T_C substantially since as shown in Ref. 13 the L2_1 -type Cr_2MnZ compounds have T_C values around room temperature.

In summary, we have studied the temperature dependence of the magnetization in HM-AFM CrMnZ ($Z = \text{P, As, Sb}$) compounds employing the many-body Green function technique. We have shown that the macroscopic magnetization in these systems does not vanish at finite temperature in contrast to the $T = 0$ limit. This anomalous behavior stems from the inequivalent magnetic sublattices in HM-AFMs which lead to different intra-sublattice exchange interactions and, as a result, spin fluctuations suppress the magnetic order of the sublattices in a different way. Thus, at finite temperatures, the sublattice magnetizations do not compensate each other and all three compounds show ferrimagnetic behavior. Moreover, the combination of large HM gaps, high T_C values and very small macroscopic magnetization around room temperature makes CrMnAs and CrMnSb promising candidates for spintronics applications.

Fruitful discussions with L. Sandratskii, I. Galanakis and Ph. Mavropoulos are greatly acknowledged.

-
- * Electronic address: e.sasioglu@fz-juelich.de
- ¹ Warren E. Pickett and Jagadeesh S. Moodera, *Physics Today* **54**, 39 (2001).
 - ² M. I. Katsnelson, V. Yu. Irkhin, L. Chioncel, and A. I. Lichtenstein, and R.A. de Groot, *Rev. Mod. Phys.* **80**, 315 (2008).
 - ³ L. M. Sandratskii and J. Kübler, *Europhys. Lett.* **33**, 447 (1996).
 - ⁴ V. V. Mazurenko, V. I. Anisimov, *Phys. Rev. B* **71**, 184434 (2005).
 - ⁵ Warren E. Pickett, *Phys. Rev. Lett.* **77**, 3185 (1996).
 - ⁶ H. van Leuken and R. A. de Groot, *Phys. Rev. Lett.* **74**, 1171 (1995).
 - ⁷ Warren E. Pickett, *Phys. Rev. B* **57**, 10613 (1998).
 - ⁸ J. H. Park, S. K. Kwon, and B. I. Min, *Phys. Rev. B* **65**, 174401 (2002).
 - ⁹ Y. K. Wang and G. Y. Guo, *Phys. Rev. B* **73**, 064424 (2006).
 - ¹⁰ M. S. Park, S. K. Kwon, and B. I. Min, *Phys. Rev. B* **64**, 100403(R) (2001).
 - ¹¹ M. Nakao, *Phys. Rev. B* **74**, 172404 (2006).
 - ¹² S. Wurmehl, H. C. Kandpal, G. H. Fecher, and C. Felser, *J. Phys.: Condens. Matter* **18**, 6171 (2006).
 - ¹³ I. Galanakis, K. Özdoğan, E. Şaşıoğlu, and B. Aktaş, *Phys. Rev. B* **75**, 172405 (2007).
 - ¹⁴ M. Nakao, *Phys. Rev. B* **77**, 134414 (2008).
 - ¹⁵ I. Galanakis, K. Özdoğan, E. Şaşıoğlu, and B. Aktaş, *Phys. Rev. B* **75**, 092407 (2007).
 - ¹⁶ D. Ködderitzsch, W. Hergert, Z. Szotek, and W. M. Temmerman, *Phys. Rev. B* **68**, 125114 (2003).
 - ¹⁷ Yung-mau Nie and Xiao Hu, *Phys. Rev. Lett.* **100**, 117203 (2008).
 - ¹⁸ H. Akai and M. Ogura, *Phys. Rev. Lett.* **97**, 026401 (2006).
 - ¹⁹ L. Bergqvist and P. H. Dederichs, *J. Phys.: Condens. Matter* **19**, 216220 (2007).
 - ²⁰ M. Ogura, C. Takahashi, and H. Akai, *J. Phys.: Condens. Matter* **19**, 365226 (2007).
 - ²¹ P. Fröbrich and P. J. Kuntz, *Physics Reports*, **432**, 223 (2006).
 - ²² S. V. Tyablikov, *Methods of Quantum Theory of Magnetism* (Plenum Press, New York, 1967).
 - ²³ E. Şaşıoğlu, L. M. Sandratskii, and P. Bruno, *Phys. Rev. B* **70**, 024427 (2004).
 - ²⁴ Among the considered compounds only CrMnSb is experimentally synthesized with a crystal structure different than the C1_b type semi-Heusler one [J. H. Wijnngaard *et al.*, *Phys. Rev. B* **45**, 5395 (1992)]. However, state-of-the-art experimental methods for the synthesis of materials such as the molecular-beam epitaxy make possible the growth of these compounds in metastable phases as thin films or multilayers where the substrate determines the lattice parameter.
 - ²⁵ I. Galanakis and Ph. Mavropoulos, *J. Phys.: Condens. Matter* **19**, 315213 (2007).
 - ²⁶ J. Ruzs, L. Bergqvist, J. Kudrnovský, and I. Turek, *Phys. Rev. B* **73**, 214412 (2006).
 - ²⁷ J. Kudrnovský, V. Drchal, I. Turek, and P. Weinberger, *Phys. Rev. B* **78**, 054441 (2008).
 - ²⁸ Ralph Skomski, *Simple Models of Magnetism*, (Oxford University Press, 2008).
 - ²⁹ P. J. Webster and K. R. A. Ziebeck, in *Alloys and Compounds of d-Elements with Main Group Elements*, Part 2,

- edited by H. R. J. Wijn, Landolt-Börnstein, New Series, Group III, Vol. 19, part. C (Springer, Berlin, 1988).
- ³⁰ H. B. Callen, Phys. Rev. **130**, 890 (1963).
- ³¹ E. Şaşıoğlu, L. M. Sandratskii, P. Bruno and I. Galanakis, Phys. Rev. B **72**, 184415 (2005).
- ³² P. A. Dowben and R. Skomski, J. Appl. Phys. **93**, 7948 (2003).
- ³³ M. Ležaić, Ph. Mavropoulos, J. Enkovaara, G. Bihlmayer, and S. Blgel Phys. Rev. Lett. **97**, 026404 (2006).
- ³⁴ J. Kübler, G. H. Fecher and C. Felser, Phys. Rev. B **76**, 024414 (2007).
- ³⁵ B. Alling, S. Shallcross, and I. A. Abrikosov, Phys. Rev. B **73**, 064418 (2006).